Optics Letters

Anti-resonant hollow-core fiber fusion spliced to laser gain fiber for high-power beam delivery

Charu Goel,† Huizi Li,† Muhammad Rosdi Abu Hassan, Wonkeun Chang, and Seongwoo Yoo*

School of Electrical and Electronics Engineering, The Photonics Institute, Nanyang Technological University, 50 Nanyang Avenue, Singapore 639798, Singapore
**Corresponding author: seon.yoo@ntu.edu.sg*

Received 8 July 2021; revised 7 August 2021; accepted 8 August 2021; posted 11 August 2021 (Doc. ID 436054); published 30 August 2021

We present the selective excitation of the fundamental mode in an anti-resonant hollow-core fiber (ARHCF) fusion-spliced with a commercial large mode area (LMA) fiber. By designing and fabricating a single-ring ARHCF that is mode-matched to a LMA fiber and by splicing the two using a CO_2 laser-based splicer, we achieve a coupling efficiency of 91.2% into the fundamental mode. We also demonstrate an all-fiber integration of an ARHCF with a commercial ytterbium-doped fiber in a laser cavity for beam delivery application. Coupling of the single-mode laser output beam into the fundamental mode of the ARHCF is demonstrated with 90.4% efficiency (<0.45 dB loss) for up to 50 W continuous wave beam in a stable and alignment-free all-fiber laser setup. © 2021 Optical Society of America

https://doi.org/10.1364/OL.436054

Hollow-core fibers (HCFs) have attracted significant research in the past two decades because of their unique characteristics [1]. Confinement of the mode field primarily to the hollow-core region in these fibers leads to low nonlinearity, ultra-low group velocity dispersion, low sensitivity to temperature, and high material damage threshold. These characteristics make HCFs attractive for the delivery of high-power laser beams [2], sensing [3], low loss transmission over ultra-wide bandwidths, and nonlinear applications like pulse compression and supercontinuum generation using gas-filled HCFs [4]. Anti-resonant hollow core fibers (ARHCFs) belong to a special class of HCFs, wherein light guidance can be explained by the principle of anti-resonant reflection in waveguides [5] and inhibited coupling of the fundamental core mode with lossy modes of dielectric cladding [6]. The negative curvature of the core boundary and the absence of dielectric nodes near the guiding modes enhance the confinement of light to the core region [7]. ARHCFs have a simpler cladding structure, compared to the photonic bandgap hollow-core fibers, and can support larger cores with an effective single-mode operation due to the orders of magnitude and higher differential propagation loss for higher order modes (HOMs) [8].

Various research groups have devoted significant research efforts toward tapping the potential of ARHCFs for laser beam delivery. There are reports on up to 300 W continuous wave (CW) power coupled into an ARHCF with a coupling efficiency of 78–81% [2] and a delivery of 7 μJ pulse with 318 kW peak power with 85% coupling efficiency [9] in free-space setups. Fusion splicing between a standard single-mode fiber (SMF) and a tapered Kagome-type anti-resonant fiber has been demonstrated in the past with 76.7% coupling efficiency into the fundamental mode with the rest coupled into the HOMs [10]. The HOMs in the ARHCF suffer high confinement losses and dissipate power thermally, leading to an increased temperature at the splice point at high powers and to possible damage [11]. Thus, it is crucial to systematically investigate low-loss fundamental mode splicing between an ARHCF and a solid-core fiber (SCF) in order to fully exploit the anticipated benefits of using the ARHCF for beam delivery. A recent report on fusion splicing ARHCFs with SMFs reported a splice loss of 1–2 dB from the SMF to the ARHCF, but it did not detail the fraction of power launched into the fundamental mode of the ARHCF [12]. In both [10,12], the splice loss in the reverse direction (from the ARHCF to the SMF) was found to be very high, e.g., 3.5 dB [10] and 10 dB [12], indicating a large-mode field mismatch between the two fibers. Authors in [13,14] have tapered single-mode solid-core fibers to match their mode field diameter (MFD) with the ARHCF and inserted the tapered SMF into the ARHCF core. This method could achieve >90% coupling into a 10 cm-long ARHCF, but the coupled power was spread over various HOMs [13]. When a high-power laser was coupled into a longer (2 m) ARHCF, where the HOMs suffer distributed filtering to the cladding region, the coupling efficiency reduced to only 40–47% [14]. Moreover, the temperature in the coating of the ARHCF rose to 110°C at a launch power of 90 W, indicating significant light leakage through the ARHCF cladding [14]. Hence, despite the prior studies, there is a significant knowledge gap in achieving a low-loss all-fiber connection with an ARHCF. This Letter reports a low-loss splicing method obtained by a customized recipe that enables a robust fundamental mode coupling between an in-house ARHCF and a commercial LMA fiber. This is achieved with an emphasis on low-loss splicing and by preserving many desired ARHCF characteristics for a fundamental mode beam delivery.

We have fabricated an ARHCF that is mode-matched to a widely used commercial large mode area solid- core fiber (LMA-SCF) with a 25 μm core size. The two fibers were fusion-spliced

using a CO_2 laser-based splicer. To achieve the lowest splice loss, we have carried out a detailed study of contributing factors—mode-field matching, cleave angle of the fiber end-face, and transverse misalignment—which are critical in deciding splicing efficiency of the LMA fibers [15]. We achieved 91.2% coupling efficiency into the fundamental mode of the ARHCF fusion spliced with the LMA-SCF. This is the first report of coupling light into the fundamental mode of an ARHCF with such high efficiency using fusion splicing. The obtained splices were found to be reciprocal, and a coupling efficiency of >90% (fundamental mode splice loss <0.45 dB) is achieved in both directions. If we take the power launched into the HOMs of the ARHCF into account, then the splice loss can be considered even lower.

The fabricated ARHCF was also spliced with a mode-matched ytterbium-doped fiber (YDF) with Fresnel reflection at the splice point forming the laser cavity. The diffraction-limited laser output beam was selectively coupled into the fundamental mode in the ARHCF with 90.4% efficiency at 50 W CW power. This is the first demonstration of integrating an ARHCF with a fiber laser cavity using fusion-splicing. In previous demonstrations [16,17], unique features of HCFs have been tapped to achieve passive mode-locking of ultrafast lasers by integrating the HCF within the laser cavity, but in free-space setups. High-efficiency fusion-splicing of the ARHCF with an active fiber reported in this Letter paves the way for environmentally stable monolithic setups for achieving the same.

The LMA-SCF fiber (LMA-GDF 25/250) considered in this work has a core diameter of 25 μm, an outer diameter (O.D.) 250 μm, a numerical aperture of 0.065, and a fundamental MFD of 19.8 μm at 1.064 μm wavelength. We have designed and fabricated a single-ring, seven-tube lattice ARHCF with a core diameter of 31 μm, an O.D. of 160 μm, a cladding capillary wall thickness of 0.78 μm and an MFD of 23.6 μm. The fiber was drawn using the standard stack-and-draw method. Figure 1 shows the scanning electron microscope (SEM) image of the fabricated fiber cross-section and the loss spectrum of its fundamental mode. The fiber exhibits a transmission loss of 0.07 dB/m at 1.064 μm. The fraction of power coupled from one fiber to another (coupling efficiency, η) in the absence of any misalignments at the splice point, is governed purely by the modal overlap given by [15]

$$\eta = \frac{\int E_1^* E_2 \mathrm{d}S}{\int E_1^* E_1 \mathrm{d}S \int E_2^* E_2 \mathrm{d}S}, \tag{1}$$

where E_1 and E_2 are the electric field amplitudes of the LMA-SCF and the ARHCF, respectively, and the surface integral is evaluated over the fiber cross-section. If the power in the LMA-SCF is significantly confined to its fundamental mode, then the fraction of power coupled into the fundamental mode of the ARHCF can be expressed in terms of the fundamental mode field diameters of the two fibers and any misalignments (transverse, longitudinal, or angular) that may occur during the splicing [15].

Figure 2(a) shows the maximum coupling efficiency achievable from the LMA-SCF to the ARHCF versus the variation in the MFD of the ARHCF, assuming flat cleaved end-faces in the two fibers and no misalignment at the splice point. We note that for the fabricated ARHCF (MFD-23.6 μm), the maximum achievable coupling efficiency between the fundamental modes is ~ 97%. Commercial splicers can ensure negligible transverse

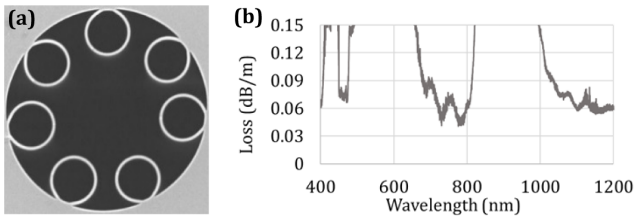

Fig. 1. (a) SEM image of the cross-section and (b) loss spectrum of the fabricated ARHCF.

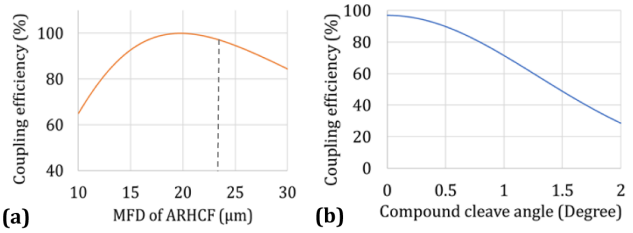

Fig. 2. Maximum achievable coupling efficiency between the fundamental modes of the LMA-SCF and the ARHCF versus (a) the MFD of the ARHCF and (b) the compound cleave angle between the two fibers assuming the MFD of the ARHCF as 23.6 μm.

and angular misalignment between the fiber end-faces while splicing. However, angular misalignment, due to the finite cleave angle of the fiber end-face, can be a decisive factor in coupling between LMA fibers [18]. Figure 2(b) shows the calculated coupling efficiency between the two fibers as a function of the compound cleave angle [16]. We note that even a 0.5° compound cleave angle can result in a significant reduction in the theoretical maximum coupling efficiency to 90% for the LMA fibers considered. One also expects an additional loss of ~ 3.3% power because of the Fresnel reflection at the interface. In our experiments, we measured the coupling efficiency as the ratio of power entering the ARHCF and exiting the SCF (and vice versa for reverse coupling), so the loss due to Fresnel reflection is accounted for in the input power itself.

The LMA-SCF and the fabricated ARHCF were spliced using a commercial CO_2 laser-based glass processing station (Fujikura LZM 100). Since the two fibers differ in their outer diameters and the ARHCF has a large air-fraction with a delicate capillary structure to preserve, the SCF is positioned closer to the splicing laser arc, and the ARHCF is given a longitudinal offset of 125 μm from the center of the arc. A laser arc power of 5.5 W is used for 1.2 ms to splice the two fibers. The splice is performed in the absence of external pressurization of capillaries, yet the fine structure in the cladding and the aspect ratio are completely preserved after splicing. The splice was strong enough to last through the rigor of the experiment, though it can be strengthened further if the O.D. of the ARHCF (160 μm) is matched with that of the LMA-SCF (250 μm). Figure 3(a) shows the longitudinal view of the splice under an optical microscope, and Fig. 3(b) shows the transverse cross-section of a broken splice point under SEM, confirming a well-preserved ARHCF structure. The fiber end-faces were cleaved using a Fujikura CT-106 cleaver that can provide repeatable cleave angles of <0.5° for both fibers. We customized the cleave parameters (clamp force and fiber tension) for the ARHCF end-face preparation.

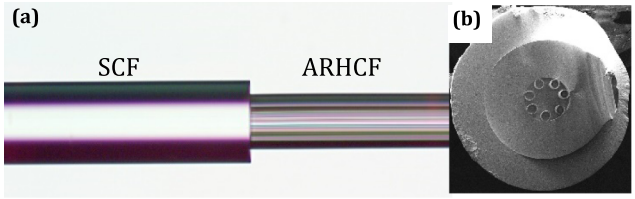

Fig. 3. (a) Longitudinal view of the splice under an optical microscope and (b) transverse view of a broken splice point under the SEM.

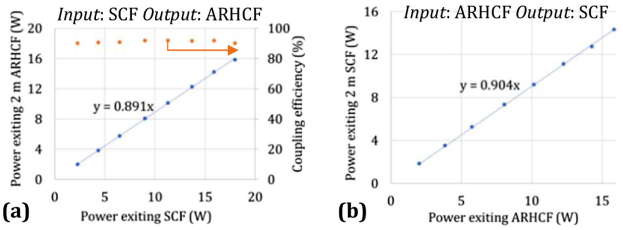

Fig. 4. (a) Power transmitted by a 2 m-long ARHCF and coupling efficiency in the fundamental mode versus power exiting the SCF. (b) Power transmitted by the SCF versus power exiting the ARHCF.

To test the coupling efficiency through the LMA-SCF and the ARHCF splice, a single-moded laser output at 1.064 μm was launched into the fundamental mode of the LMA-SCF using a suitable mode-field adaptor, and the power transmitted by the 2 m-long spliced ARHCF was measured. Figure 4(a) shows the power exiting the ARHCF as a function of the power exiting the SCF at the splice point. The transmission efficiency (ratio of power exiting the ARHCF to the power exiting the SCF) was measured to be 89.1%, corresponding to a coupling efficiency of 91.2% after considering the transmission loss (0.07 dB/m) of the fiber, as per Fig. 1(b). The beam quality of the light exiting the ARHCF was characterized by $M^2 < 1.05$, confirming the transmitted light to be in the fundamental mode of the ARHCF. The cleave angles for this splice were 0.1° for the SCF and 0.2° for the ARHCF, resulting in a compound cleave angle mismatch of 0.3°. Considering the effects of the cleave angle, the mode-field mismatch, and no other misalignment, the expected maximum theoretical coupling efficiency between the power exiting the SCF and that entering ARHCF is ∼ 94%, which is a good match with the observed value.

The propagation loss of the spliced ARHCF was measured by cutting back 1 m of fiber length, and the measured value was matched with the independent measurement of the propagation loss of the fundamental mode in the long length of the ARHCF [Fig. 1(b)]. This confirms that only the fundamental mode propagated in the spliced ARHCF. The HOMs in the fabricated ARHCF are expected to propagate with at least >0.3 dB/m loss in our numerical simulations performed using the full-vector finite-element modeling in COMSOL Multiphysics. Any core HOMs excited at the splice point would lose their thermal power as they propagate along the fiber. The temperature at and near the splice point remained <30°C for a launched power of up to 18 W, confirming low power lost, and hence an efficient fundamental mode coupling. The power output was unaffected by bending the ARHCF down to a bending diameter of 20 cm.

To further improve the coupling efficiency, we tested tapering the input end of the ARHCF to reduce its MFD to match better with the LMA-SCF. The tapered ARHCF retained its original

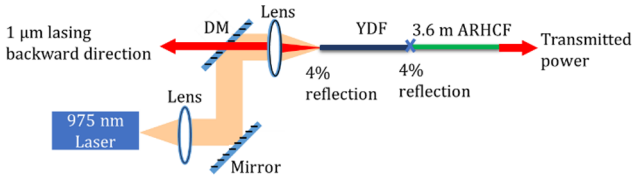

Fig. 5. Integrating a spliced ARHCF with a YDF laser cavity. DM: Dielectric mirror reflecting 975 nm and transmitting wavelengths >1000 nm.

capillary fine-structure and resulted in an improvement in coupling efficiency by 2%, which is in-line with the theoretical prediction. To test the reciprocity of the splice, another piece of the LMA-SCF (2 m long) was spliced at the output end of the ARHCF, and the power transmitted through it was measured. The transmission efficiency through LMA-SCF was measured to be 90.4%, as shown in Fig. 4(b). Since the SCF in this length scale has negligible transmission loss, the coupling efficiency can be assumed to be the same as the transmission efficiency in this case. The excellent reciprocity of the splice loss is aligned with the theory and provides an easy technique for selectively exciting the fundamental mode in an LMA-SCF that otherwise supports 12 guided core modes.

The successful low loss splicing method was transferred to a fiber laser cavity. The ARHCF was spliced with a commercial YDF (Nufern YDF-25/250-VIII) having the same fiber dimensions as the LMA-SCF considered in the previous section. A 4%–4% linear laser cavity was built as per the experimental setup shown in Fig. 5. The cleave angles for both fibers at the splice point were 0.2°. Fresnel reflection at the glass-air interface at the input end of the YDF and at the splice point with the ARHCF formed the laser cavity. The laser cavity was cladding-pumped with a diode laser at 975 nm. Any residual pump power at the splice point would not propagate through the ARHCF because of the strong mode mismatch between the pump light and the ARHCF core modes. Moreover, 975 nm lies in the resonant band of the ARHCF and would suffer high propagation loss in the fiber. Therefore, the power transmitted out of the ARHCF is purely the laser output, which was also confirmed by the measurement of the output spectrum using the optical spectrum analyzer.

The YDF was coiled with 8.5 cm bend diameter, and both of its end-faces were flat cleaved with a cleave angle of 0.2°, leading to a symmetric cavity. In the absence of the spliced ARHCF, the laser output from the YDF was characterized by a slope efficiency of 47.6% and $M^2_{\text{mean}} = 1.07$ in both the forward and backward directions with less than 1% difference in power levels. Therefore, in these experiments, we have simultaneously measured the power and beam quality for the beam exiting the ARHCF and for the laser output in the backward direction (pump input end of YDF). Figure 6(a) shows the power transmitted through a 3.6 m-long ARHCF versus a variation in laser output power. The transmission efficiency is found to be 85.3%, corresponding to a coupling efficiency of 90.4% into the fundamental mode for a CW power of 50.2 W. Consistent coupling efficiency was observed across the available laser power, as presented in Fig. 6(a). Figure 6(b) shows the beam quality measurement of the transmitted beam through the ARHCF, which is characterized by $M^2_{x,y} = 1.01$ and 1.00, respectively. The slight improvement in M^2 after propagation through the

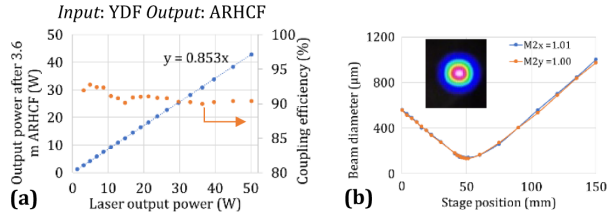

Fig. 6. (a) Power transmitted through the 3.6 m-long ARHCF and coupling efficiency versus laser output power and (b) the M^2 measurement of the transmitted beam. Inset: Mode profile of output beam.

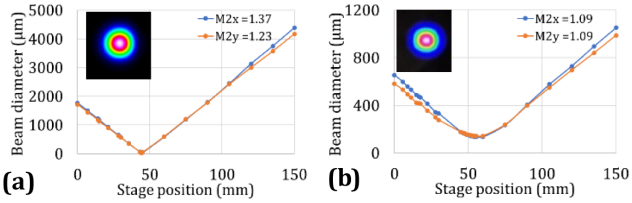

Fig. 7. M^2 measurement of (a) direct laser output and (b) beam exiting the ARHCF.

ARHCF is the result of filtering any HOMs that were present in the coupled laser beam.

To investigate this effect further and to show its potential application in spatial filtering of the laser beam to improve beam quality, we adjusted the YDF bend so that the laser output is characterized by a higher $M^2_{\text{mean}} = 1.30$ [Fig. 7(a)] without the ARHCF. In this configuration, the transmission efficiency through the ARHCF drops down to 81.5% for a coupled power of 52.2 W because of the higher loss suffered by HOMs in the ARHCF. The power exiting the ARHCF is characterized by $M^2_{\text{mean}} = 1.09$ [Fig. 7(b)], which clearly implies that propagation through an ARHCF can improve the beam quality at the cost of some power loss. We should mention that the ARHCF used was not specifically fabricated for HOM suppression, and its higher order mode extinction ratio (HOMER) is only ~ 6 for the first HOM. Hence, the HOMs are not completely suppressed within the given length. By designing the capillary diameter ~ 0.68 times the core diameter, a HOMER that is greater than 1000 can be obtained in an ARHCF without affecting the propagation loss in the fundamental mode [8]. We believe such fibers are suitable candidates for high power laser beam delivery. We plan to investigate further in this direction by fabricating an ARHCF with a high HOMER and explore its potential for improving the laser beam quality as a spatial mode filter [19].

In summary, we reported the first demonstration of >90% coupling efficiency into the fundamental mode of a single-ring ARHCF using fusion splicing with a solid core fiber. We discussed the effects of mode matching and cleave angle on coupling efficiency. The same design principles can be extended to any larger mode area ARHCF, as well as nested anti-resonant fibers. The spliced ARHCF is also integrated in a YDF laser cavity for beam delivery through fusion splicing. We achieved low loss and efficient laser beam delivery with a coupling efficiency of 90.4% for launched powers of over 50 W. Although our experiments were constrained to a CW laser, we believe that the operating principle holds for the delivery of ultrashort pulses as well. Direct splicing of an active fiber with an ARHCF opens potential avenues for utilizing the modal characteristics of the ARHCF for enhancing the performance of high-power CW and ultrafast pulsed fiber lasers.

Funding. National Research Foundation Singapore (QEP-P4).

Disclosures. The authors declare no conflicts of interest.

Data Availability. Data underlying the results presented in this paper are not publicly available at this time but may be obtained from the authors upon reasonable request.

[†]These authors contributed equally to this Letter.

REFERENCES

1. M. Komanec, D. Dousek, D. Suslov, and S. Zvanovec, Radioengineering **29**, 417 (2020).
2. X. Zhu, D. Wu, Y. Wang, F. Yu, Q. Li, Y. Qi, J. Knight, S. Chen, and L. Hu, Opt. Express **29**, 1492 (2021).
3. C. Goel, J. Zang, M. Parrot, and S. Yoo, J. Lightwave Technol. **39**, 3998 (2021).
4. B. Debord, F. Amrani, L. Vincetti, F. Gérôme, and F. Benabid, Fibers **7**, 16 (2019).
5. M. A. Duguay, Y. Kokubun, T. L. Koch, and L. Pfeiffer, Appl. Phys. Lett. **49**, 13 (1986).
6. L. Vincetti and V. Setti, Opt. Express **18**, 23133 (2010).
7. W. Belardi and J. C. Knight, Opt. Express **21**, 21912 (2013).
8. P. Uebel, M. C. Günendi, M. H. Frosz, G. Ahmed, N. N. Edavalath, J.-M. Ménard, and P. St.J. Russell, Opt. Lett. **41**, 1961 (2016).
9. M. Michieletto, J. K. Lyngsø, C. Jakobsen, J. Lægsgaard, O. Bang, and T. T. Alkeskjold, Opt. Express **24**, 7103 (2016).
10. X. Zheng, B. Debord, L. Vincetti, B. Beaudou, F. Gérôme, and F. Benabid, Opt. Express **24**, 14642 (2016).
11. I. A. Bufetov, A. N. Kolyadin, A. F. Kosolapov, V. P. Efremov, and V. E. Fortov, Opt. Express **27**, 18296 (2019).
12. Y. Min, A. Filipkowski, G. Stępniewski, D. Dobrakowski, J. Zhou, B. Lou, M. Klimczak, L. Zhao, and R. Buczyński, J. Lightwave Technol. **39**, 3251 (2021).
13. W. Huang, Y. Cui, X. Li, Z. Zhou, Z. Li, M. Wang, X. Xi, Z. Chen, and Z. Wang, Opt. Express **27**, 37111 (2019).
14. W. Huang, X. Ye, Y. Cui, Z. Zhou, Z. Chen, Z. Wang, and J. Chen, in *Proc. SPIE* **11849**, Fourth International Symposium on High Power Laser Science and Engineering (2021), paper 118490I.
15. A. Ghatak and K. Thyagarajan, *An Introduction to Fiber Optics* (Cambridge University, 1998).
16. C. M. Harvey, F. Yu, J. C. Knight, W. J. Wadsworth, and P. J. Almeida, IEEE Photon. Technol. Lett. **28**, 669 (2016).
17. H. Lim, A. Chong, and F. W. Wise, Opt. Express **13**, 3460 (2005).
18. N. Simakov, A. V. Hemming, A. Carter, K. Farley, A. Davidson, N. Carmody, M. Hughes, J. M. O. Daniel, L. Corena, D. Stepanov, and J. Haub, Opt. Express **23**, 3126 (2015).
19. P. Patimisco, A. Sampaolo, L. Mihai, M. Giglio, J. Kriesel, D. Sporea, G. Scamarcio, F. K. Tittel, and V. Spagnolo, Sensors **16**, 533 (2016).